ACS OMEGA

http://pubs.acs.org/journal/acsodf

Article

Autocitrullination and Changes in the Activity of Peptidylarginine Deiminase 3 Induced by High Ca^{2+} Concentrations

Mizuki Sawata, Hiroki Shima, Kazutaka Murayama, Toshitaka Matsui, Kazuhiko Igarashi, Kazumasa Funabashi, Kenji Ite, Kenji Kizawa, Hidenari Takahara, and Masaki Unno*

Cite This: *ACS Omega* 2022, 7, 28378−28387

Read Online

ACCESS | Metrics & More | Article Recommendations | Supporting Information

ABSTRACT: Peptidylarginine deiminases (PADs) are enzymes that catalyze the Ca^{2+}-dependent conversion of arginine residues into proteins to citrulline residues. Five PAD isozymes have been identified in mammals. Several studies have shown that the active-site pockets of these isozymes are formed when Ca^{2+} ions are properly bound. We previously characterized the structures of PAD3 in six states. Among these, we identified a "nonproductive" form of PAD3 in which the active site was disordered even though five Ca^{2+} ions were bound. This strange structure was probably obtained as a result of either high Ca^{2+} concentration (~260 mM)-induced denaturation during the crystallization process or high Ca^{2+}-concentration-induced autocitrullination. While autocitrullination has been reported in PAD2 and PAD4 for some time, only a single report on PAD3 has been published recently. In this study, we investigated whether PAD3 catalyzes the autocitrullination reaction and identified autocitrullination sites. In addition to the capacity of PAD3 for autocitrullination, the autocitrullination sites increased depending on the Ca^{2+} concentration and reaction time. These findings suggest that some of the arginine residues in the "nonproductive" form of PAD3 would be autocitrullinated. Furthermore, most of the autocitrullinated sites in PAD3 were located near the substrate-binding site. Given the high Ca^{2+} concentration in the crystallization condition, it is likely that Arg372 was citrullinated in the "nonproductive" PAD3 structure, the structure was slightly altered from the active form by citrulline residues, and probably inhibited Ca^{2+}-ion binding at the proper position. Following Arg372 citrullination, PAD3 enters an inactive form; however, the Arg372-citrullinated PAD3 are considered minor components in autocitrullinated PAD3 (CitPAD3), and CitPAD3 does not significantly decrease the enzyme activity. Autocitrullination of PAD3 could not be confirmed at the low Ca^{2+} concentrations seen *in vivo*. Future experiments using cells and animals are needed to verify the effect of Ca^{2+} on the PAD3 structure and functions *in vivo*.

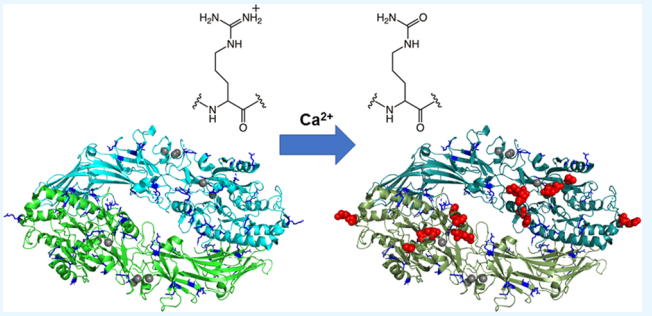

INTRODUCTION

The deimination of arginine residues into citrulline residues is an important post-translational protein modification (Figure 1). Replacing the positive charges of the protein molecule with neutral ones causes changes in the protein conformation and intramolecular and/or intermolecular interactions.[1−4] This post-translational modification promotes myelin sheath formation, which results in the keratinization of the epidermis as well as hair and the insulating effect of nerve axons.[5] Conversely, abnormalities in this post-translational modification can cause various diseases, such as rheumatoid arthritis and multiple sclerosis.[5−9]

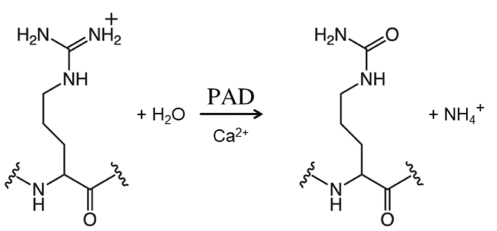

Figure 1. Citrullination reaction catalyzed by peptidylarginine deiminases.

Protein citrullination is catalyzed by peptidylarginine deiminases (PADs), which are Ca^{2+}-dependent enzymes (Figure 1). Five PAD isozymes have been identified in mammals, PAD1-PAD4 (663−665 residues long) and PAD6 (690 residues long), with a similar molecular weight (approximately 75 kDa per monomer) and a sequence identity

Received: May 12, 2022
Accepted: July 18, 2022
Published: August 8, 2022

of approximately 50%. However, their tissue localization, substrates, and associated diseases differ.[10−13]

To date, only the structures of PAD1, PAD2, PAD3, and PAD4 have been elucidated using X-ray crystallography.[14−17] Interestingly, PAD3 and PAD4 bind five Ca^{2+} ions per monomer,[14,18] whereas PAD1 and PAD2 bind four and six Ca^{2+} ions per monomer, respectively.[15,16] Furthermore, it has been suggested that Ca^{2+}-ion binding to PADs leads to the formation of their active-site pocket, which allows substrate or inhibitor binding;[14,15,18] *i.e.*, some Ca^{2+} ions serve as switches activating the enzyme function of PADs.

PAD3 is a unique PAD isozyme as it exhibits the highest substrate specificity.[19,20] In neural stem cells, cell death is induced upon PAD3-mediated citrullination of apoptosis-inducing factor, thus suggesting that PAD3 acts as an upstream regulator of Ca^{2+}-dependent cell death.[21] Furthermore, PAD3 plays important roles in hair follicle formation by citrullinating trichohyalin, an arginine-rich structural protein abundant in the inner root sheath and medulla.[22,23] In addition, S100A3, a Ca^{2+}-binding protein that abundantly localizes in cuticular cells, was shown to be a PAD3 substrate.[24] PAD3- and S100A3-associated hair keratinization responses began to occur in mammals during evolution.[25] Mutations in the PAD3 gene are reported to be the cause of uncombable hair syndrome.[26,27]

We have recently elucidated the structures of PAD3 in six states and reported them in a previous paper.[18] These structures included the ligand-free wild-type (WT) PAD3 (Apo WT PAD3, PDB ID; 7D4Y), the active form of PAD3 in which Ca^{2+} ions bind to the appropriate sites (WT PAD3-Ca^{2+}, PDB ID; 7D5V), the "nonproductive" PAD3 form in which Ca^{2+} binds to inappropriate sites ("nonproductive" WT PAD3-Ca^{2+}, PDB ID; 7D8N), the inhibitor-bound form in which both Ca^{2+} and the general PAD inhibitor Cl-amidine are bound (WT PAD3-Ca^{2+}-Cl-amidine, PDB ID; 7D56), the C646A mutant of PAD3 in which catalytic residue Cys646 is substituted by alanine (C646A PAD3, PDB ID; 7D5V), and the C646A mutant structure with Ca^{2+} ions bound to it (C646A PAD3-Ca^{2+}, PDB ID; 7D5R). In the "nonproductive" WT PAD3-Ca^{2+}, in the vicinity of Ca2, one of the five Ca^{2+}-binding sites, Asp369 and Arg372 formed a salt bridge that prevented Ca^{2+} binding to the appropriate site.[18] This was thought to be an adverse effect of co-crystallization at a very high Ca^{2+} concentration (260 mM), which is not attainable *in vivo*.

It has been reported that PAD2 and PAD4 catalyze autocitrullination reactions in the presence of Ca^{2+}.[28−31] Recently, autocitrullination of PAD3 was also identified and the sites were reported.[32] Since the "nonproductive" WT PAD3-Ca^{2+} was crystallized in the presence of a very high Ca^{2+} concentration (260 mM),[18] we also considered the possibility that the obtained structure underwent autocitrullination. In the present study, we independently examined whether PAD3 catalyzes autocitrullination in the presence of high Ca^{2+} concentrations and attempted to identify the autocitrullination sites. In addition, the effect of autocitrullination on the structure and activity of PAD3 is discussed.

RESULTS AND DISCUSSION

PAD3 Is Autocitrullinated. WT PAD3 (3 mg/mL) incubated for 3 h at 37 °C with a reaction buffer solution containing either 10 mM $CaCl_2$ or 1 mM EDTA (as a control) was subjected to two-dimensional (2D) electrophoresis. Proteins transferred onto a poly vinylidene difluoride (PVDF) membrane were detected using SYPRO ruby stain and specific antibodies for PAD3. Total protein staining of WT PAD3 with EDTA showed a major spot at the position of isoelectric point (pI) 6.3. The same spot was also probed by a specific antibody for PAD3 with rather tailed patterns (Figure 2). Control PAD3 migrated with a slight basic nature

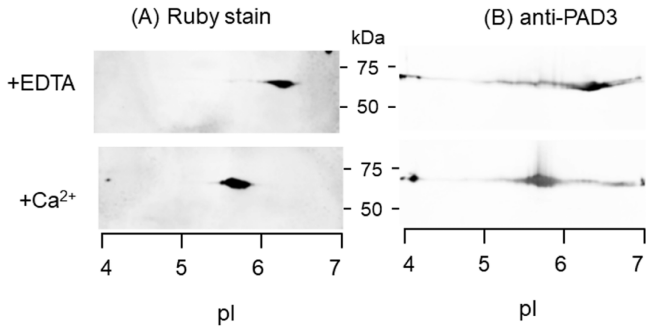

Figure 2. Acidic shift of autocitrullinated PAD3. Aliquots (3 μg each) incubated in the presence of either EDTA (control experiment) or Ca^{2+} and subjected to 2D electrophoresis. Protein transferred onto a PVDF membrane was stained with SYPRO ruby for the detection of total protein (A) and subsequently probed with anti-PAD3 antibody (B).

compared to the theoretical pI 5.7 computed by Expacy (Swiss Institute of Bioinformatics) for the His-tagged actual construct of the WT PAD3 sequence. Conversely, the spots of PAD3 incubated with $CaCl_2$ were detected at the apparently shifted acidic side (pI 5.6−5.8). The reduction of pI value could be simulated by substituting approximately half of the 39 arginine residues of PAD3 with citrullines. These results suggest that a number of sites of PAD3 were preferentially autocitrullinated.

PAD3 Autocitrullination Is Ca^{2+}-Concentration-Dependent. When PAD3 was incubated with various $CaCl_2$ concentrations (0, 0.5, 1.0, 2.0, and 4.0 mM) at 37 °C for 4 h, we discovered that the autocitrullination was taking place above a $CaCl_2$ concentration of 2 mM (Figure 3). The results

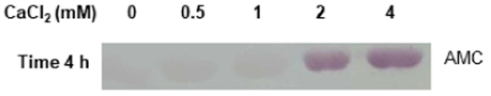

Figure 3. Ca^{2+}-concentration-dependent autocitrullination of PAD3 detected using western blotting. A primary antibody against AMC was used to detect PAD3 peptidylcitrulline. The PAD3 concentration used was 0.1 mg/mL. The autocitrullination reaction of PAD3 was performed for 4 h. Anti-modified citrulline (AMC); peptidylarginine deiminase 3 (PAD3).

of band quantification using ImageJ also showed that the relative concentrations were 1.0, 1.0, 1.1, 5.3, and 6.0 when incubated with 0, 0.5, 1.0, 2.0, and 4.0 mM $CaCl_2$, respectively, and autocitrullination was quantitatively evaluated from a $CaCl_2$ concentration of 2 mM (Supporting Table S1).

Autocitrullination Is Dependent on the Reaction Time. The Ca concentration was next fixed at 4 mM, and the reaction times were varied. The results showed that the peptidylcitrulline levels increased in a reaction-time-dependent manner (Figure 4, top). Furthermore, we confirmed that the concentration of PAD3 remained constant during this process

https://doi.org/10.1021/acsomega.2c02972
ACS Omega 2022, 7, 28378−28387

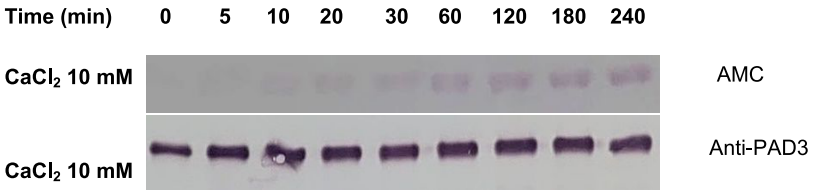

Figure 4. Reaction-time-dependent changes in the citrulline levels at stable PAD3 concentrations detected using western blotting. In the upper figure, an anti-AMC primary antibody was used to detect the autocitrullinated PAD3. In the lower figure, an anti-PAD3 primary antibody was used to detect PAD3 (PAD3 concentration: 0.05 mg/mL; $CaCl_2$ concentration during the PAD3 autocitrullination reaction: 10 mM). Anti-modified citrulline (AMC); peptidylarginine deiminase 3 (PAD3).

(Figure 4, bottom). Bands quantification using ImageJ allowed us to further show that the citrullination levels increased in a reaction-time-dependent manner, while the concentrations of PAD3 remained unchanged (Figure 5 and Supporting Table S2).

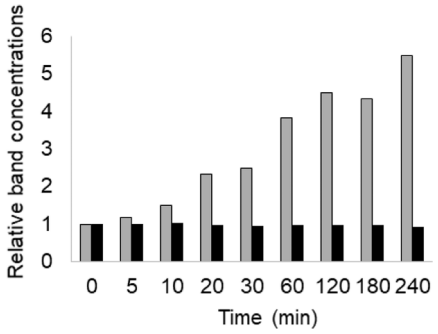

Figure 5. Quantification of the citrulline concentration based on western blotting quantification (Figure 4). The horizontal axis represents time in minutes. The vertical axis represents the relative value of the band intensity of 0 min as 1. Gray bars and black bars represent the relative band concentrations for AMC and anti-PAD3, respectively. Anti-modified citrulline (AMC); peptidylarginine deiminase 3 (PAD3).

To confirm the specific binding of the primary antibody, S100A3, gel filtration buffer, gel filtration buffer + $CaCl_2$, BSA, conalbumin, aldolase, and molecular weight markers were used as controls (see Methods). As a result, small control bands representing proteins other than S100A3 citrullinated by PAD3 were identified, indicating that the primary antibody hardly bound nonspecifically.

Autocitrullination of PAD3 was confirmed to occur in a Ca^{2+} concentration (>2 mM)- and reaction-time (>1 h)-dependent manner using western blotting.

Activity of Autocitrullinated PAD3. The activities of purified WT PAD3, putative autocitrullinated PAD3 (CitPAD3; WT PAD3 incubated with Ca^{2+}), and PAD3 C646A mutant (C646A), in which the catalytic residue Cys646 was substituted by alanine, were compared. The activities were calculated based on the absorption at 490 nm (A_{490}). A reaction time of 10 min was used due to the reliable absorbance within 1.0. The activity of CitPAD3 was shown to be 20% lower than that of WT PAD3 (Figure 6).

Identification of Autocitrullinated Sites. First, we attempted to identify the sites of autocitrullination using matrix-assisted laser desorption ionization time-of-flight mass spectrometry (MALDI-TOF MS). In this experiment, we detected the difference in the molecular weight of arginine, a basic amino acid, and citrulline, a neutral amino acid, to identify the citrullination sites. During MALDI-TOF MS,

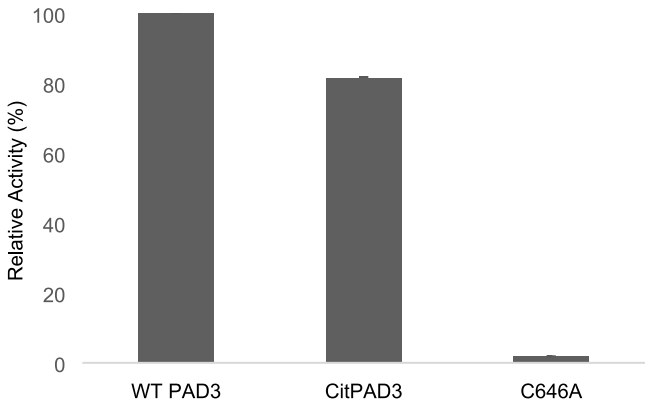

Figure 6. PAD3 activity. From left to right: activity measurements (n = 3) of WT PAD3 (37 °C, 1 h incubation without Ca^{2+}), CitPAD3 (37 °C, 1 h incubation with 10 mM $CaCl_2$), and PAD3 C646A mutant. The vertical axis indicates the activity percentage of WT PAD3 as 100%, based on the formula shown in Identification of Autocitrullinated Sites. Peptidylarginine deiminase 3 (PAD3); wild type (WT).

trypsin treatment cleaves proteins at the position behind basic amino acids. The different residues are detected based on the differentially cleaved fragments. For the CitPAD3 sample, the peptide containing citrulline(s) was detected in a state not cleaved by trypsin. We searched for "1-missing fragments found only in CitPAD3" and the results showed that Arg346 and Arg440 were candidates. However, the corresponding fragments sometimes appeared in both WT PAD3 and CitPAD3 or sometimes in neither of them. Therefore, the autocitrullination sites could not be identified in this experiment using MALDI-TOF MS.

Next, we attempted to identify autocitrullinated sites using liquid chromatography−MS (LC-MS)/MS. Four measurements were conducted on samples prepared under various conditions (see the Methods section). Table 1 lists the peptide fragments containing arginine(s) or citrulline(s) identified in the four experiments (duplicates were omitted). The percentages of amino acids in PAD3 identified using LC-MS/MS are summarized in Supporting Table S3, while the sites containing arginine identified using LC-MS/MS are listed in Table 2. Citrullination was observed in some cases and not in others, even at the same Ca^{2+} concentrations and reaction times. It is unclear whether this is due to differences in equipment, protein purification L. O. T., or minor differences in sample preparation procedures. Nine sites in PAD3, Arg131, Arg343, Arg346, Arg372, Arg394, Arg397, Arg399, Arg447, and Arg510, were identified as probable autocitrullination sites. Arg314 was detected in both WT PAD3 without Ca^{2+} and C646A, the inactive mutant. Since these two states of PAD3

https://doi.org/10.1021/acsomega.2c02972
ACS Omega 2022, 7, 28378−28387

Table 1. Peptide Fragments Containing Arginine(s) and/or Citrulline(s) of Trypsin-Treated PAD3 Identified Using Liquid Chromatography−Mass Spectrometry/Mass Spectrometry (LC-MS/MS)

confirmed arginine	peptides identified using LC-MS/MS	Mr (expt/calc)
Arg131 → Cit	129 QDCitNFVDK 136	1028.4840/1028.429
Arg131 → Cit	129 QDCitNFVDKR 137	1177.5850/1177.5840
Arg137		
Arg137	138 QWVWGPSGYGGILLVNCDR 156	2190.6780/2190.0681
Arg156		
Arg186	157 DDPSCDVQDNCDQHVHCLQDLEDMSVMVLR 186	3671.5461/3671.5419
		3687.5353/3687.5361 (+oxidation)
Arg186	187 TQGPAALFDDHK 198	1298.6249/1298.6255
Arg210	210 RAQVFHICGPEDVCEAYR 227	2234.0380/2234.0361
Arg227		
Arg210	211 AQVFHICGPEDVCEAYR 227	2077.9365/2077.9350
Arg227		
Arg241	235 VSYEVPR 241	848.4391/848.4392
Arg312	293 VAPWIMTPSTLPPLEVYVCR 312	2342.2171/2342.2167
		2358.2162/2358.2116 (+oxidation)
Arg314 → Cit	313 VCitNNTCFVDAVAELAR 328	1848.9160/1848.9152
Arg328		
Arg328	315 NNTCFVDAVAELAR 328	1592.7636/1592.7617
Arg343	334 LTICPQAENR 343	1214.6089/1214.6077
Arg343 → Cit	334 LTICPQAENCitND R346	1585.6760/1585.7631
Arg343 → Cit	334 LTICPQAENCitNDCitWIQDEMELGYVQAPHK 362	3526.6631/3526.6609
Arg346 → Cit		
Arg346	347 WIQDEMELGYVQAPHK 362	1942.9255/1942.9247
Arg372	363 TLPVVFDSPR 372	1129.6139/1129.6132
Arg372 → Cit	363 TLPVVFDSPCitNGELQDFPYKR 383	1129.5370/1129.6132
Arg383	373 NGELQDFPYKR 383	1365.6678/1365.6677
Arg394	384 ILGPDFGYVTR 394	1236.6506/1236.6503
Arg394 → Cit	384 ILGPDFGYVTCitEPR 397	1619.8320/1619.8308
Arg397 → Cit	395 EPCitDCitSVSGLDSFGNLEVSPPVVANGK 421	2827.4004/2827.3988
Arg399 → Cit		
Arg399 → Cit	398 DCitSVSGLDSFGNLEVSPPVVANGK 421	2444.2199/2444.2183
Arg399	400 SVSGLDSFGNLEVSPPVVANGK 421	2172.1068/2172.1063
Arg427	400 SVSGLDSFGNLEVSPPVVANGKEYPLGR 427	2888.5884/2888.4556
Arg399 → Cit	398 DCitSVSGLDSFGNLEVSPPVVANGKEYPLGR 427	2444.3514/2444.2183
Arg427	428 ILIGGNLPGSSGR 440	1239.6938/1239.6935
Arg440		
Arg447 → Cit	442 VTQVVCitDFLHAQK 454	1540.8371/1540.8362
Arg510 → Cit	506 CGHGCitALLFQGVVDDEQVK 524	2142.0547/2142.0528
Arg552	543 FVQSCIDWNR 552	1337.6197/1337.6187
Arg557	558 ELGLAECDIIDIPQLFK 574	1987.0347/1987.0336
Arg652	619 SLLEPLGLHCTFIDDFTPYHMLHGEVHCGTNVCR 652	4066.9070/4066.8951

cannot catalyze autocitrullination, Arg314 must be a false positive. The citrullinated arginine residues in the PAD3 molecule accounted for 23% (9/39) of the total arginine residues. This result supported our 2D electrophoresis results, in which the sample was prepared by reacting with Ca^{2+} for a sufficient time and at a sufficient concentration.

However, certain sites remained undetectable using LC-MS/MS (Tables 1 and 2, and Supporting Table S3). In addition, autocitrullination was not confirmed at Ca^{2+} concentrations observed *in vivo* (tens of nM at steady state and hundreds of nM transiently, rising to 1 mM during citrullination of S100A3; Figure 3).[24,33] Therefore, if autocitrullination of PAD3 occurs *in vivo* remains unknown and should be investigated in the future.

Characteristics of Autocitrullinated Sites in PAD3. The autocitrullinated sites of PAD3 are shown in Figure 7. Nine of the 39 arginine residues were autocitrullinated in PAD3, with a high concentration at the substrate-binding site and near Ca2 (Figure 8). Previously, Arg372 was thought to form a salt bridge with Asp369 in the "nonproductive" WT PAD3-Ca^{2+}.[18] However, in this study, Arg372 was autocitrullinated in the presence of high Ca^{2+} concentrations; thus, its interaction with Asp369 was hypothesized to be a hydrogen bond rather than a salt bridge as previously suggested.

Comparison of Autocitrullinated Sites with Those in the Other Isozymes. Autocitrullination has also been observed in PAD2 as well as PAD4,[13,28−30] and the percentage of autocitrullinated sites in PAD2 and PAD4 accounted for 48% (16/33) and 70% (19/27) of the total arginine residues, respectively (Table 3). The citrullination rate of PAD3 is the lowest among the three isozymes (23%), thus suggesting that this correlates with the higher substrate specificity of PAD3.[20,34]

https://doi.org/10.1021/acsomega.2c02972
ACS Omega 2022, 7, 28378−28387

Table 2. Regions Containing Arginine or Citrulline Detected Using Liquid Chromatography−Mass Spectrometry/Mass Spectrometry[a]

	experiment 1				experiment 2						experiment 3			experiment 4
	(1)	(2)	(3)	(4)	(5)	(6)	(7)	(8)	(9)	(10)	(11)	(12)	(13)	(14)
Arg131	N	√	√	√	N	N	N	N	N	N	N	√	N	√
Arg314	√	N	N	√	N	N	N	N	N	N	N	N	×	N
Arg343	×	N	N	√	×	×	×	×	×	×	×	√	×	√
Arg346	×	N	N	√	×	×	×	×	×	×	×	×	×	×
Arg372	×	×	×	√	×	×	×	×	×	×	×	×	×	×
Arg394	×	√	√	×	×	×	×	×	×	×	×	×	×	×
Arg397	N	√	√	N	N	N	N	N	N	N	N	N	N	N
Arg399	N	√	√	√	N	N	N	N	N	N	N	√	×	√
Arg427	N	N	N	N	N	N	N	N	N	N	√	N	√	√
Arg447	N	N	√	N	N	N	N	N	N	N	N	N	N	N
Arg510	N	√	√	√	N	N	N	N	N	N	N	N	N	N

[a] √, the identified citrullinated arginine moiety; ×, the noncitrullinated arginine site identified; N, the arginine site not detected in the experiment. The experiments were conducted four times. The L. O. T. of WT PAD3 samples are different from each other. However, for the third and fourth measurements, the L. O. T. of WT PAD3 samples were identical (see Table 1).

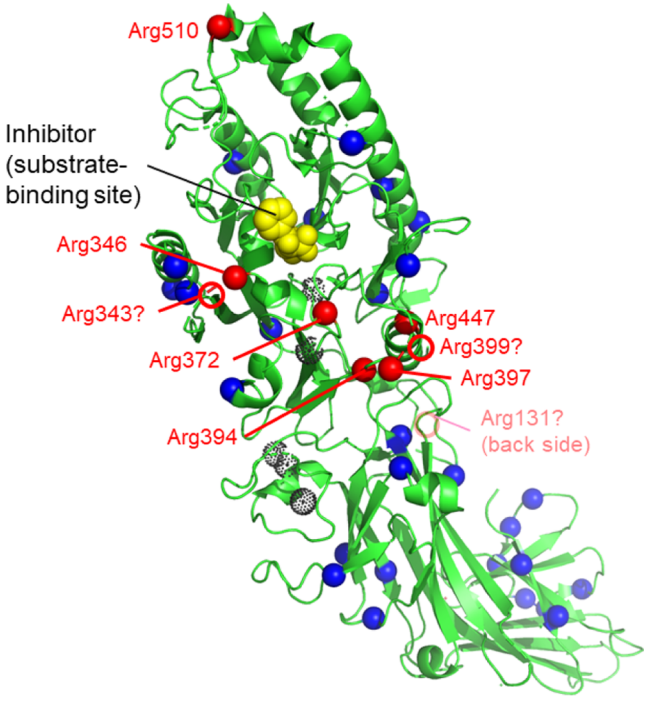

Figure 7. Distribution of arginine and citrullinated arginine residues in PAD3. The structure of WT PAD3-Ca^{2+}-Cl-amidine (Chain A of PDB ID; 7D56) is shown in green. The dotted black spheres indicate Ca^{2+} ions. Blue and red spheres indicate arginine and autocitrullinated arginine residues, respectively. In 7D56, six of the nine citrullinated arginine residues were visualized. Red circles indicate three autocitrullinated arginine residues (Arg131, Arg343, and Arg399) at putative positions that were not identified following the X-ray crystallographic structure analysis. The inhibitor Cl-amidine is shown in yellow. Peptidylarginine deiminase 3 (PAPD3); wild type (WT).

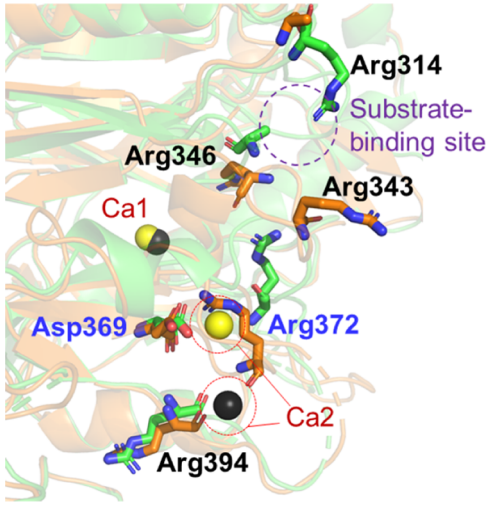

Figure 8. Close-up view of citrullines distribution near the substrate-binding site. The structures of WT PAD3-Ca^{2+} and the "non-productive" WT PAD3-Ca^{2+} are shown in green and orange, respectively. Yellow and black spheres indicate Ca^{2+} in the WT PAD3-Ca^{2+} structure and the "nonproductive" WT PAD3-Ca^{2+} structure, respectively. The structure of Arg343 in the WT PAD3-Ca^{2+} was not determined. The purple dotted circle indicates the vicinity with the substrate-binding site. Peptidylarginine deiminase 3 (PAD3); wild type (WT).

Structural comparison of autocitrullination sites among PAD isozymes revealed that autocitrullination sites differed among PAD isozymes: in PAD2 and PAD4, potentially citrullinated arginine residues were evenly distributed throughout the molecular structure, whereas in PAD3, autocitrullination sites were concentrated around the substrate-binding site (Figures 9 and 7). This result suggests that PAD3 more selectively recognizes only flexible regions in the substrates, in this case its own substrate-binding sites.

We also examined whether there are common autocitrullinated residues among the different isozymes. The results showed that Arg372 near Ca2 was commonly autocitrullinated (Figure 10). In addition, Arg394 was shown to be commonly autocitrullinated in PAD3 and PAD4, although it was not common in PAD2 (Table 4). These results suggest that Arg372 is one of the residues to be autocitrullinated.

Arg372-Citrullinated PAD3 Is Inactive and Different From CitPAD3 Which Retains Certain Activity. The presence of Ca^{2+} increases the activity of PADs by a factor of >10,000.[35] As previously mentioned, PAD enzymes are thought to become active following Ca^{2+}-ion binding to the appropriate sites, forming the active site.[14,15,18] The results of this study suggest that Arg372 of the "nonproductive" WT

https://doi.org/10.1021/acsomega.2c02972
ACS Omega 2022, 7, 28378−28387

Table 3. Arginine Residues in PAD3 and Those in PAD2 and PAD4 that Have Been Reported to Be Autocitrullinated

reference	arginine residues that can be citrullinated
PAD3 (this work)	131, 343, 346, 372, 394, 397, 399, 447, 510
PAD1[32]	5, 41, 56, 58, 67, 93, 140, 217, 240, 290, 310, 345, 348, 374, 376, 385, 396, 442, 446, 449, 489, 525, 534, 538, 551, 556, 650, 651
PAD2[28]	3, 5, 8, 68, 78, 168, 187, 344, 373, 428, 441, 442, 525, 582, 652, 653
PAD2[32]	8, 14, 54, 126, 157, 168, 187, 193, 344, 373, 395, 441, 448, 546, 552, 580, 582, 619, 652, 653
PAD3[32]	62, 67, 227, 241, 328, 343, 346, 372, 383, 394, 399, 427, 440, 447, 487, 510 552, 557, 652
PAD4[31]	123, 156, 205, 419, 484, 609, 639
PAD4[29]	205, 212, 218, 372, 374, 383, 394, 495, 536, 544
PAD4[30]	8, 123, 131, 137, 156, 205, 212, 218, 292, 372, 374, 383, 394, 419, 427, 441, 484, 488, 495, 536, 544, 550, 555, 609, 639, 650, 651
PAD4[28]	372, 374, 383, 394, 441, 550, 639
PAD4[32]	123, 205, 212, 218, 292, 372, 374, 383, 394, 419, 441, 484, 488, 495, 536, 544, 555, 609, 639, 651

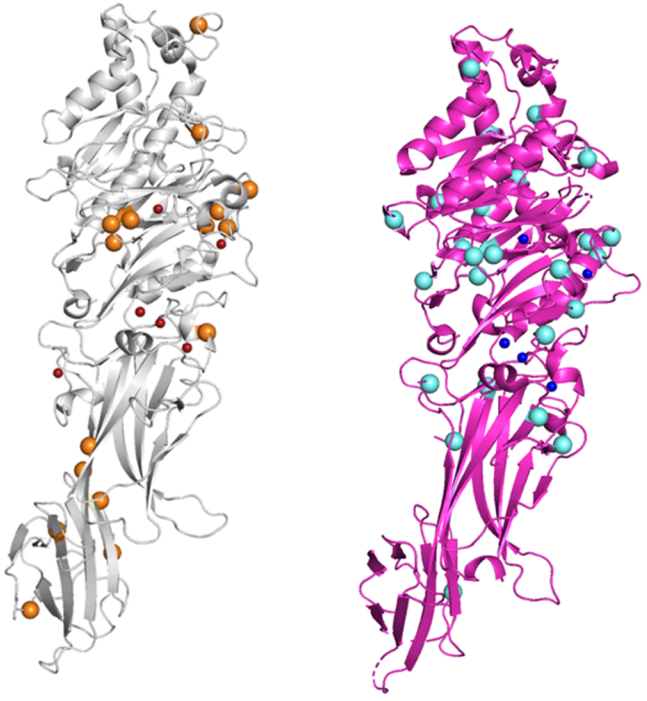

Figure 9. Potential autocitrullinated sites of PAD isozymes. (Left) Structure of PAD2-Ca^{2+} (PDB ID; 4N2C), depicted in a gray cartoon model. The small red and large orange spheres represent Ca^{2+} ions and arginine residues which are supposed to be autocitrullinated, respectively. (Right) Structure of PAD4-Ca^{2+} (PDB ID; 1WD9), depicted in a magenta cartoon model. The small blue and large cyan spheres represent Ca^{2+} ions and the arginine residues which are supposed to be autocitrullinated, respectively. Unlike the distribution of citrullinated arginine residues in PAD3 (shown in Figure 7), the arginine residues to be citrullinated appear to be uniformly distributed throughout the structure of PAD2-Ca^{2+} and PAD4-Ca^{2+}. Peptidylarginine deiminase (PAD); wild type (WT).

PAD3-Ca^{2+} reported in a previous study[18] is likely to be citrullinated. Furthermore, the enzyme activity measurements in this study indicate that the activity of CitPAD3 is not substantially decreased by autocitrullination. However, the structure of the active site in the "nonproductive" WT PAD3-Ca^{2+} was not formed due to disorder.[18] At a first glance, these

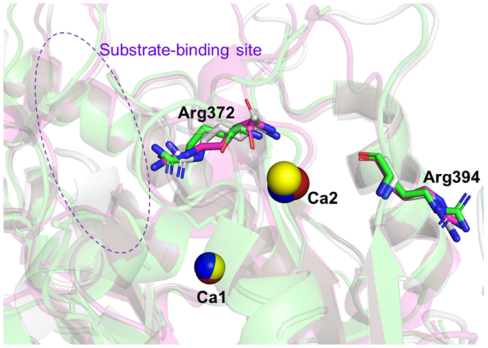

Figure 10. Structures around Arg372, which is citrullinated in PAD2, PAD3, and PAD4, and Arg394, which is citrullinated in PAD3 and PAD4.[28,30] The structures of PAD2, PAD3, and PAD4 are all Ca^{2+}-bound forms and colored in gray, green, and magenta, respectively. Only Arg372 and Arg394 (PAD3 numbering) are depicted in stick models, in which the N and O atoms are colored in blue and red, respectively. The Ca^{2+} (Ca1 and Ca2) ions bound in the vicinity of the two arginine residues of interest are depicted as red, yellow, and blue spheres in the PAD2, PAD3, and PAD4 structures, respectively. The purple dotted circle indicates the vicinity of the substrate-binding site. PAD, peptidylarginine deiminase.

results appear to be contradictory. Clues to explain this discrepancy in the structure and activity of the CitPAD3 may be identified in the results of activity and citrullination measurements of Arg372 in PAD4. It has been reported that Arg372 in PAD4 is autocitrullinated (Table 3).[28−30,32] In addition, PAD4 whose Arg372 is genetically engineered to citrulline significantly lost its activity.[36] Conversely, the autocitrullination reaction of PAD4 showed small effects on the activity,[31] similar to that reported regarding PAD3 in this study. Careful analysis has indicated that in PAD4, Arg372 (and Arg374) is (are) citrullinated to lesser degrees than other arginine residues.[36] Given that PAD3 is an isozyme similar to PAD4 in structure and substrate recognition,[18] these facts suggest that even in PAD3, Arg372 might be citrullinated under certain conditions, although to a lesser extent than other sites. This is also strongly suggested by the fact that citrullination of Arg372 in PAD3 was only observed in one of our experiments under various conditions (Table 2). Considering that the crystal structure of the "nonproductive" WT PAD3-Ca^{2+} was analyzed from crystals obtained under using high (260 mM) Ca^{2+} concentration conditions,[18] the absence of active-site formation following Arg372 citrullination is in agreement with the experimental results for PAD4, in which the activity was significantly decreased. The structure of the "nonproductive" WT PAD3-Ca^{2+} represents the inactive form.[18] This is considered to be a state in which Arg372 is citrullinated, preventing the formation of the active site. Alternatively, we believe that the rate of citrullination of Arg372 is not high in CitPAD3 (based on the PAD4 result and Table 2)[36] as Arg372 is considered to be citrullinated under extreme conditions or by chance, but seldom citrullinated under biochemical conditions. Activity measurements have been performed under 10 mM $CaCl_2$ and 1 h incubation conditions. In contrast, the crystallization condition of "nonproductive" WT PAD3-Ca^{2+} contained 260 mM $CaCl_2$, five days to one week was necessary to crystallize PAD3. Hence, in the PAD3 autocitrullination experiments, few PAD3 molecules were Arg372-citrullinated although, if Arg372 undergoes citrullination, the molecule itself should be almost

https://doi.org/10.1021/acsomega.2c02972
ACS Omega 2022, 7, 28378−28387

Table 4. Samples and Their Preparation for LC-MS/MS[a]

LC-MS/MS experiment number		samples	Ca^{2+} concentration (mM)	incubation time (min)	EDTA (mM)	desalting after incubation with Ca^{2+}
1	(1)	WT-1	0	0	1.0	
	(2)	WT-1	4	120	1.0	yes
	(3)	WT-1	4	120	1.0	no
	(4)	WT-1	10	30	1.0	no
2	(5)	WT-2	10	0		no
	(6)	WT-2	10	30		no
	(7)	WT-2	10	60		no
	(8)	WT-2	10	120		no
	(9)	C646A	0	0		
	(10)	C646A	10	120		no
3	(11)	WT-3	0	0		
	(12)	WT-3	10	960		no
	(13)	C646A	10	960		no
4	(14)	WT-3	10	96		no

[a]LC-MS/MS, liquid chromatography−mass spectrometry/mass spectrometry; WT, wild type.

inactive. Therefore, supporting the result indicates that the enzymatic activity of CitPAD3 was not severely reduced by this process (Figure 6).

CONCLUSIONS

Autocitrullination was confirmed in PAD3, and it was shown to be Ca^{2+}-concentration- and reaction-time-dependent. LC-MS/MS showed that nine arginine residues of PAD3 can be autocitrullinated under high Ca^{2+} concentrations. Furthermore, the number of autocitrullination sites increased in a Ca^{2+} concentration- and reaction-time-dependent manner. In PAD3, most autocitrullination sites were located near the substrate-binding site, suggesting that the flexible sites in the molecular structure were recognized and citrullinated. Arg372 was autocitrullinated when exposed to a high concentration of Ca^{2+} for a long time, indicating that the residue could be citrulline in the structure of the "nonproductive" WT PAD3-Ca^{2+}.[18] The activity of autocitrullinated PAD3 (CitPAD3) was 20% lower than that of WT PAD3; however, the enzyme activity was not completely lost. This suggests that the structure of the "nonproductive" WT PAD3-Ca^{2+} represents an inactive form and that the Arg372 of PAD3 is citrullinated in the presence of an extremely high Ca^{2+} concentration (260 mM) when it is allowed to undergo crystallization for a long time, whereas Arg372 of PAD3 is hardly citrullinated after approximately 1 h of incubation with ∼10 mM Ca^{2+}.[36] In other words, although CitPAD3 contains the inactive PAD3 molecules with Arg372 citrullinated, they are considered to be fairly minor components under biochemical conditions. PAD3 had the lowest autocitrullination rate compared to those of PAD2 and PAD4, which is likely to correlate with the results of our experiments showing that PAD3 had the highest substrate specificity.

METHODS

PAD3 and S100A3 Gene Expression and Protein Purification. Human PAD3 (WT and C646A mutant)[17,18] and human S100A3[37] gene expression and protein purification were performed as previously described.

Activity Assay. The activity assay was performed using a previously reported method.[38] First, 100 μL of PAD3 solution diluted in 20 mM Tris-HCl (pH 7.2) was added to 250 μL of reaction mixture (100 mM Tris-HCl [pH 7.2], 10 mM $CaCl_2$, 10 mM DTT, 10 mM *Nα*-benzoyl-L-arginine ethyl ether [BAEE]) and heated at 55 °C for 0−60 min in a block incubator. Then, 50 μL of 8 M HCl was added to stop the reaction. Next, 100 μL of redox buffer containing 0.278 M $NH_4Fe(SO_4)_2{\cdot}12H_2O$, 0.278 M $(NH_4)_2Fe(SO_4)_2{\cdot}6H_2O$, and 0.5 M H_2SO_4 was added and heated in a block incubator at 100 °C for 10 min. After incubating at room temperature for 10 min, 500 μL of mixed acid (distilled water: H_3PO_4:H_2SO_4 = 2:3:1 in volume) and 200 μL of diacetyl monoxime solutions were added and heated at 100 °C for 20 min. After incubating at room temperature for 10 min, spectra were measured using a UV−visible spectrophotometer (V-650 JASCO Corporation). The colorimetric changes of citrulline at 490 nm[39] relative to those of BAEE were calculated, and the spectral changes for each reaction time were tabulated. All heating reactions were carried out under light-shielded conditions. The final concentration of PAD3 was unified to approximately 50 nM, and the activity of PAD3 was defined using the following equation:

$$\text{activity} = \frac{\text{abs (490 nm) at 10 min}}{\text{protein concentration (nM)}}$$

The $CaCl_2$ concentration in the reaction mixture ranged from 0 to 200 mM (final concentration). For the citrullinated PAD3 (CitPAD3), the sample of WT PAD3 (0.05 mg/mL) was first reacted with 10 mM $CaCl_2$ at 37 °C for 1 h in a block incubator. For WT PAD3, the $CaCl_2$ concentration was 0 mM and the other conditions were the same (37 °C for 1 h) as those for CitPAD3. Next, the reacted PAD3 sample was diluted to a concentration of 0.01 mg/mL (50 nM) and the activity was measured.

For the activity measurements, little or no autocitrullination of PAD3 occurred due to the excessive amount of artificial substrate (BAEE, 10 mM) relative to the enzyme (PAD3, 50 nM) in the 10 min reaction time.

2D Electrophoresis. Samples were prepared by incubating WT PAD3 (3 mg/mL) in 20 mM Tris-HCl buffer (pH 7.6) containing 500 mM NaCl, 10% (v/v) glycerol, and 5.0 mM DTT and either 1 mM EDTA (Control experiment) or 10 mM $CaCl_2$ at 37 °C for 3 h. The reaction was stopped, and free thiol groups of the protein were blocked by mixing with an equal volume of 1 M iodoacetamide dissolved in 3 M Tris-Cl (pH 8.5). After incubation for 15 min at room temperature, samples were centrifugally de-salted and proteins were diluted in the rehydration buffer (5.6 M urea, 1.6 M thiourea, 1.6%

https://doi.org/10.1021/acsomega.2c02972
ACS Omega 2022, 7, 28378−28387

CHAPS, 20 mM DTT in Bio-Lyte ampholytes 3−10 buffer [Bio-Rad, Hercules, CA]). Samples were loaded onto an immobilized pH-gradient strip with a pH range of 4−7 (ReadyStrip, Bio-Rad) and rehydrated overnight. Isoelectric focusing was performed at 200 V for 20 min, 450 V for 15 min, 750 V for 15 min, and 2000 V for 30 min. Two-dimension electrophoresis was performed with a precast 4−12% NuPAGE Bis-Tris Zoom gel using 3-morpholinopropanesulfonic acid (MOPS)-SDS buffer.

Two-dimensionally separated proteins were transferred onto a PVDF membrane (Invitrogen, Waltham, MA). Total protein transferred onto the PVDF membrane was stained with SYPRO Ruby protein blot stain (Molecular Probes, Eugene, OR) according to the manufacturer's protocol. Fluorescence signals of total protein were detected by an Amersham Imager 600 using 520 nm light with Cy3 filter (Green mode). Subsequently, the PVDF membrane was subjected to immunofluorescence labeling of PAD3 with rabbit anti-PAD3 antibody (Abcam, Cambridge, MA; ab50246) followed by AlexaFluor488-labeled goat anti-rabbit IgG (Invitrogen). Immunofluorescence signal from the same PVDF membrane was detected using a 460 nm light with Cy2 filter (Blue mode).

Western Blotting. First, Ca^{2+} was (or was not) added to PAD3 and the mixture was incubated at 37 °C. Then, to stop the reaction, the PAD3 solution was mixed with 4× sample buffer (4× sample buffer: PAD3 solution = 6:18 μL) and incubated at 95 °C for 5 min. Then, 6 μL of the mixture was separated using SDS-PAGE. The 4× sample buffer consisted of 0.25 M Tris-HCl (pH 6.8), 8% (w/v) SDS, 20% (v/v) sucrose, 20% (v/v) 2-mercaptoethanol, and 0.008% (w/v) bromophenol blue (BPB). The SDS-PAGE gel consisted of 9 or 12% acrylamide gel. A 13 or 15% acrylamide gel and Tris-Tricine buffer were used when S100A3 was used as control.

Western blotting of one-dimensional (1D) PAGE gel was conducted using Immun-Blot Goat Anti-Rabbit IgG (H + L)-AP Assay Kit (Bio-Rad) according to the manufacturer's instructions with slight modifications. The equipment used was PowerPac Basic (Bio-Rad).

To detect peptidylcitrullines using an anti-citrullinated protein detection kit (anti-modified citrulline [AMC], Merck & Co. Inc., Kenilworth, NJ), the membrane was soaked in citrulline chemical modification solution (Regent I [3.8 M H_2SO_4, 3.7 M H_3PO_4, 1.5 mM $FeCl_3 \cdot 6H_2O$]: Regent II [2% diacetyl monoxime, 1% antipyrine, 1 M acetic acid] = 2:1) with the transferred side down, and was shaken overnight at 45 rpm and 37 °C (Bioshaker, BR-23FP, TAITEC, Saitama, Japan). A control experiment using a 1,000-fold dilution of the Anti-PAD3 antibody with Tris-Buffered Saline with Tween20 as the primary antibody was also conducted.

As controls, S100A3, and S100A3 citrullinated by PAD3, gel filtration buffer, gel filtration buffer + Ca^{2+}, BSA (66.5 kDa) (Fujifilm Wako Pure Chemical Corporation, Osaka, Japan), conalbumin (75 kDa; Merck), aldolase (158 kDa; Merck), and a molecular weight marker (Precision Plus Protein, #1610363, Bio-Rad) were used. The final washed membrane was dried using a hair dryer. Quantification of western blot band densities was performed using ImageJ.

Liquid Chromatography−Mass Spectrometry/Mass Spectrometry (LC-MS/MS). Samples were prepared by adding various concentrations (0, 4, and 10 mM) of $CaCl_2$ to PAD3 solutions (WT or C646A) and incubated in a block incubator at 37 °C for 30−960 min (Table 4). Samples (1−4) were stored at −80 °C until used for LC-MS/MS measurements. The rest of the samples (5−14) were mixed with 4× sample buffer immediately after the incubation with $CaCl_2$ at 37 °C was completed, then incubated in a block incubator at 95 °C for 5 min to be denatured, and subjected to SDS-PAGE. The sample solutions in samples 1−4 contained EDTA, while the sample solutions in samples 5−14 did not. For sample 2, salts were removed using a desalting column (HiTrap Desalting, Cytiva, Tokyo, Japan). The presence or absence of EDTA does not affect the activity measured by the activity assay using BAEE. After electrophoresis, the gel was washed with ultrapure water for 5 min while shaking, stained with the CBB staining solution for 10 min, and further washed with ultrapure water overnight. The CBB-stained gel areas were cut out using a scalpel and proteins in the excised gel areas were reduced using 100 mM DTT and alkylated using 100 mM iodoacetamide or acrylamide. The gel pieces were then subjected to in-gel digestion using trypsin overnight at 37 °C for samples 1−4 or 30 °C for samples 5−14. The digested peptides from each sample were treated with a ZipTip (Millipore, Billerica, MA) for mass spectrometry analysis, and loaded onto a fused-silica capillary column containing C18 resin (Nikkyo Technos, Tokyo, Japan) with a diameter of 75 μm and length of 10 cm. The peptides were eluted with an acetonitrile gradient (typically 2.4 to 22% in 46 min, then to 33% in 49 min) in 0.1% formic acid. LC-MS/MS samples 1−4 were analyzed using an Orbitrap Fusion mass spectrometer equipped with an EASY-nLC 1000 high-performance liquid chromatography (HPLC) system (Thermo Fisher Scientific Inc., Waltham, MA). Samples 5−14 were analyzed by Japan Proteomics Co., Ltd., using a DiNa HPLC system (KYA TECH Corporation, Tokyo, Japan) and QSTAR XL (Applied Biosystems, Foster City, CA). Database searches were performed against Swissprot and a homemade list of common contaminating proteins using the MASCOT ver. 2.5.1 search engine (Matrix Science, London, U.K.). The MASCOT searches were carried out for tryptic peptides using 5 ppm peptide mass tolerance and 0.5 Da MS/MS tolerance. Oxidation (+15.9949 Da), propionamide (+71.0371 Da), and citrullination (+0.9840 Da) were considered as modifications for Met, Cys, and Arg, respectively.

■ ASSOCIATED CONTENT

Supporting Information

The Supporting Information is available free of charge at https://pubs.acs.org/doi/10.1021/acsomega.2c02972.

Quantification of citrulline concentration based on band intensity from western blotting experiments and $CaCl_2$ concentration dependence (Table S1), $CaCl_2$ incubation time dependence (Table S2), and protein sequence coverage in LC-MS/MS experiment (Table S3) (PDF)

Accession Codes

Uniprot Q9ULW8

■ AUTHOR INFORMATION

Corresponding Author

Masaki Unno − *Graduate School of Science and Engineering, Ibaraki University, Hitachi 316-8511, Japan; Frontier Research Center for Applied Atomic Sciences, Ibaraki University, Naka 319-1106, Japan;* orcid.org/0000-0002-4975-5696; Phone: +81-294-38-5041; Email: masaki.unno.19@vc.ibaraki.ac.jp

https://doi.org/10.1021/acsomega.2c02972
ACS Omega 2022, 7, 28378−28387

Authors

Mizuki Sawata − *Graduate School of Science and Engineering, Ibaraki University, Hitachi 316-8511, Japan*

Hiroki Shima − *Department of Biochemistry, Tohoku University Graduate School of Medicine, Sendai 980-8575, Japan*

Kazutaka Murayama − *Graduate School of Biomedical Engineering, Tohoku University, Sendai 980-8579, Japan;* orcid.org/0000-0003-1749-4038

Toshitaka Matsui − *Institute of Multidisciplinary Research for Advanced Materials, Tohoku University, Sendai 980-8577, Japan;* orcid.org/0000-0003-3865-8468

Kazuhiko Igarashi − *Department of Biochemistry, Tohoku University Graduate School of Medicine, Sendai 980-8575, Japan*

Kazumasa Funabashi − *Graduate School of Science and Engineering, Ibaraki University, Hitachi 316-8511, Japan*

Kenji Ite − *Graduate School of Science and Engineering, Ibaraki University, Hitachi 316-8511, Japan*

Kenji Kizawa − *Kao Corporation, Biological Science Research Laboratory, Odawara 250-0002, Japan*

Hidenari Takahara − *College of Agriculture, Ibaraki University, Inashiki 300-0393, Japan; Frontier Research Center for Applied Atomic Sciences, Ibaraki University, Naka 319-1106, Japan*

Complete contact information is available at: https://pubs.acs.org/10.1021/acsomega.2c02972

Funding

This work was mainly supported by MEXT KAKENHI (grant numbers JP25121704 and JP23121504) and partly supported by JSPS KAKENHI (grant number JP19K06507).

Notes

The authors declare no competing financial interest.

■ ACKNOWLEDGMENTS

The authors thank Nihon Proteomics, Inc. for their efforts in some of the LC-MS/MS measurements. They are grateful to Dr. Kenichi Kitanishi, Ms. Makiko Ishihara (Industry-Academia-Government Collaboration Researchers), Mr. Shimpei Tashima, and the members, including past members, of their laboratory for their advice. They thank ATTO Corporation for lending them the 2D electrophoresis equipment for the preliminary experiment. This work was performed under the Cooperative Research Program of the "Network Joint Research Center for Materials and Devices."

■ REFERENCES

(1) Christophorou, M. A.; Castelo-Branco, G.; Halley-Stott, R. P.; Oliveira, C. S.; Loos, R.; Radzisheuskaya, A.; Mowen, K. A.; Bertone, P.; Silva, J. C. R.; Zernicka-Goetz, M.; Nielsen, M. L.; Gurdon, J. B.; Kouzarides, T. Citrullination regulates pluripotency and histone H1 binding to chromatin. *Nature* **2014**, *507*, 104−108.

(2) Jones, J. E.; Causey, C. P.; Knuckley, B.; Slack-Noyes, J. L.; Thompson, P. R. Protein arginine deiminase 4 (PAD4): Current understanding and future therapeutic potential. *Curr. Opin. Drug Discov. Devel.* **2009**, *12*, 616−627.

(3) Slade, D. J.; Subramanian, V.; Thompson, P. R. Citrullination unravels stem cells. *Nat. Chem. Biol.* **2014**, *10*, 327−328.

(4) Vossenaar, E. R.; Zendman, A. J. W.; van Venrooij, W. J.; Pruijn, G. J. M. PAD, a growing family of citrullinating enzymes: Genes, features and involvement in disease. *BioEssays* **2003**, *25*, 1106−1118.

(5) Jones, J. E.; Slack, J. L.; Fang, P.; Zhang, X.; Subramanian, V.; Causey, C. P.; Coonrod, S. A.; Guo, M.; Thompson, P. R. Synthesis and screening of a haloacetamidine containing library to identify PAD4 selective inhibitors. *ACS Chem. Biol.* **2012**, *7*, 160−165.

(6) Chang, X.; Han, J.; Pang, L.; Zhao, Y.; Yang, Y.; Shen, Z. Increased PADI4 expression in blood and tissues of patients with malignant tumors. *BMC Cancer* **2009**, *9*, No. 40.

(7) McElwee, J. L.; Mohanan, S.; Griffith, O. L.; Breuer, H. C.; Anguish, L. J.; Cherrington, B. D.; Palmer, A. M.; Howe, L. R.; Subramanian, V.; Causey, C. P.; Thompson, P. R.; Gray, J. W.; Coonrod, S. A. Identification of PADI2 as a potential breast cancer biomarker and therapeutic target. *BMC Cancer* **2012**, *12*, No. 500.

(8) Witalison, E.; Thompson, P.; Hofseth, L. Protein arginine deiminases and associated citrullination: Physiological functions and diseases associated with dysregulation. *Curr. Drug Targets* **2015**, *16*, 700−710.

(9) Suzuki, A.; Yamada, R.; Chang, X.; Tokuhiro, S.; Sawada, T.; Suzuki, M.; Nagasaki, M.; Nakayama-Hamada, M.; Kawaida, R.; Ono, M.; Ohtsuki, M.; Furukawa, H.; Yoshino, S.; Yukioka, M.; Tohma, S.; Matsubara, T.; Wakitani, S.; Teshima, R.; Nishioka, Y.; Sekine, A.; Iida, A.; Takahashi, A.; Tsunoda, T.; Nakamura, Y.; Yamamoto, K. Functional haplotypes of PADI4, encoding citrullinating enzyme peptidylarginine deiminase 4, are associated with rheumatoid arthritis. *Nat. Genet.* **2003**, *34*, 395−402.

(10) Klareskog, L.; Rönnelid, J.; Lundberg, K.; Padyukov, L.; Alfredsson, L. Immunity to citrullinated proteins in rheumatoid arthritis. *Annu. Rev. Immunol.* **2008**, *26*, 651−675.

(11) Harauz, G.; Musse, A. A. A tale of two citrullines—structural and functional aspects of myelin basic protein deimination in health and disease. *Neurochem. Res.* **2007**, *32*, 137−158.

(12) Kim, J. K.; Mastronardi, F. G.; Wood, D. D.; Lubman, D. M.; Zand, R.; Moscarello, M. A. Multiple sclerosis. *Mol. Cell. Proteomics* **2003**, *2*, 453−462.

(13) Slack, J. L.; Causey, C. P.; Thompson, P. R. Protein arginine deiminase 4: A target for an epigenetic cancer therapy. *Cell. Mol. Life Sci.* **2011**, *68*, 709−720.

(14) Arita, K.; Hashimoto, H.; Shimizu, T.; Nakashima, K.; Yamada, M.; Sato, M. Structural basis for Ca^{2+}-induced activation of human PAD4. *Nat. Struct. Mol. Biol.* **2004**, *11*, 777−783.

(15) Slade, D. J.; Fang, P.; Dreyton, C. J.; Zhang, Y.; Fuhrmann, J.; Rempel, D.; Bax, B. D.; Coonrod, S. A.; Lewis, H. D.; Guo, M.; Gross, M. L.; Thompson, P. R. Protein arginine deiminase 2 binds calcium in an ordered fashion: Implications for inhibitor design. *ACS Chem. Biol.* **2015**, *10*, 1043−1053.

(16) Saijo, S.; Nagai, A.; Kinjo, S.; Mashimo, R.; Akimoto, M.; Kizawa, K.; Yabe-Wada, T.; Shimizu, N.; Takahara, H.; Unno, M. Monomeric form of peptidylarginine deiminase type I revealed by x-ray crystallography and small-angle x-ray scattering. *J. Mol. Biol.* **2016**, *428*, 3058−3073.

(17) Unno, M.; Kizawa, K.; Ishihara, M.; Takahara, H. Crystallization and preliminary x-ray crystallographic analysis of human peptidylarginine deiminase type III. *Acta Crystallogr., Sect. F: Struct. Biol. Cryst. Commun.* **2012**, *68*, 668−670.

(18) Funabashi, K.; Sawata, M.; Nagai, A.; Akimoto, M.; Mashimo, R.; Takahara, H.; Kizawa, K.; Thompson, P. R.; Ite, K.; Kitanishi, K.; Unno, M. Structures of human peptidylarginine deiminase type III provide insights into substrate recognition and inhibitor design. *Arch. Biochem. Biophys.* **2021**, *708*, No. 108911.

(19) Kizawa, K.; Takahara, H.; Troxler, H.; Kleinert, P.; Mochida, U.; Heizmann, C. W. Specific citrullination causes assembly of a globular S100A3 homotetramer. *J. Biol. Chem.* **2008**, *283*, 5004−5013.

(20) Méchin, M. C.; Enji, M.; Nachat, R.; Chavanas, S.; Charveron, M.; Ishida-Yamamoto, A.; Serre, G.; Takahara, H.; Simon, M. The peptidylarginine deiminases expressed in human epidermis differ in their substrate specificities and subcellular locations. *Cell. Mol. Life Sci.* **2005**, *62*, 1984−1995.

(21) U, K. P.; Subramanian, V.; Nicholas, A. P.; Thompson, P. R.; Ferretti, P. Modulation of calcium-induced cell death in human neural stem cells by the novel peptidylarginine deiminase−AIF pathway. *Biochim. Biophys. Acta, Mol. Cell Res.* **2014**, *1843*, 1162−1171.

(22) Méchin, M.-C.; Sebbag, M.; Arnaud, J.; Nachat, R.; Foulquier, C.; Adoue, V.; Coudane, F.; Duplan, H.; Schmitt, A.-M.; Chavanas, S.; Guerrin, M.; Serre, G.; Simon, M. Update on peptidylarginine deiminases and deimination in skin physiology and severe human diseases. *Int. J. Cosmet. Sci.* **2007**, *29*, 147−168.
(23) Nachat, R.; Méchin, M.-C.; Charveron, M.; Serre, G.; Constans, J.; Simon, M. Peptidylarginine deiminase isoforms are differentially expressed in the anagen hair follicles and other human skin appendages. *J. Invest. Dermatol.* **2005**, *125*, 34−41.
(24) Kizawa, K.; Takahara, H.; Unno, M.; Heizmann, C. W. S100 and S100 fused-type protein families in epidermal maturation with special focus on S100A3 in mammalian hair cuticles. *Biochimie* **2011**, *93*, 2038−2047.
(25) Minato, T.; Unno, M.; Kitano, T. Evolution of S100A3 and PAD3, two important genes for mammalian hair. *Gene* **2019**, *713*, No. 143975.
(26) Ü Basmanav, F. B.; Cau, L.; Tafazzoli, A.; Méchin, M.-C.; Wolf, S.; Romano, M. T.; Valentin, F.; Wiegmann, H.; Huchenq, A.; Kandil, R.; Garcia Bartels, N.; Kilic, A.; George, S.; Ralser, D. J.; Bergner, S.; Ferguson, D. J. P.; Oprisoreanu, A.-M.; Wehner, M.; Thiele, H.; Altmüller, J.; Nürnberg, P.; Swan, D.; Houniet, D.; Büchner, A.; Weibel, L.; Wagner, N.; Grimalt, R.; Bygum, A.; Serre, G.; Blume-Peytavi, U.; Sprecher, E.; Schoch, S.; Oji, V.; Hamm, H.; Farrant, P.; Simon, M.; Betz, R. C. Mutations in three genes encoding proteins involved in hair shaft formation cause uncombable hair syndrome. *Am. J. Hum. Genet.* **2016**, *99*, 1292−1304.
(27) Hsu, C.-K.; Romano, M. T.; Nanda, A.; Rashidghamat, E.; Lee, J. Y. W.; Huang, H.-Y.; Songsantiphap, C.; Lee, J. Y.-Y.; Al-Ajmi, H.; Betz, R. C.; Simpson, M. A.; McGrath, J. A.; Tziotzios, C. Congenital anonychia and uncombable hair syndrome: coinheritance of homozygous mutations in RSPO4 and PADI3. *J. Invest. Dermatol.* **2017**, *137*, 1176−1179.
(28) Darrah, E.; Davis, R. L.; Curran, A. M.; Naik, P.; Chen, R.; Na, C. H.; Giles, J. T.; Andrade, F. Citrulline not a major determinant in the recognition of peptidylarginine deiminase 2 and 4 by autoantibodies in rheumatoid arthritis. *Arthritis Rheumatol.* **2020**, *72*, 1476−1482.
(29) Andrade, F.; Darrah, E.; Gucek, M.; Cole, R. N.; Rosen, A.; Zhu, X. Autocitrullination of human peptidyl arginine deiminase type 4 regulates protein citrullination during cell activation. *Arthritis Rheumatol.* **2010**, *62*, 1630−1640.
(30) Liu, X.; Wichapong, K.; Lamers, S.; Reutelingsperger, C. P. M.; Nicolaes, G. A. F. Autocitrullination of PAD4 does not alter its enzymatic activity: In vitro and in silico studies. *Int. J. Biochem. Cell Biol.* **2021**, *134*, No. 105938.
(31) Slack, J. L.; Jones, L. E.; Bhatia, M. M.; Thompson, P. R. Autodeimination of protein arginine deiminase 4 alters protein−protein interactions but not activity. *Biochemistry* **2011**, *50*, 3997−4010.
(32) Maurais, A. J.; Salinger, A. J.; Tobin, M.; Shaffer, S. A.; Weerapana, E.; Thompson, P. R. A streamlined data analysis pipeline for the identification of sites of citrullination. *Biochemistry* **2021**, *60*, 2902−2914.
(33) Lewis, R. S. Store-operated calcium channels: New perspectives on mechanism and function. *Cold Spring Harbor Perspect. Biol.* **2011**, *3*, No. a003970.
(34) Unno, M.; Kawasaki, T.; Takahara, H.; Heizmann, C. W.; Kizawa, K. Refined Crystal Structures of human Ca^{2+}/Zn^{2+}-binding S100A3 protein characterized by two disulfide bridges. *J. Mol. Biol.* **2011**, *408*, 477−490.
(35) Mondal, S.; Thompson, P. R. Protein arginine deiminases (PADs): Biochemistry and chemical biology of protein citrullination. *Acc. Chem. Res.* **2019**, *52*, 818−832.
(36) Mondal, S.; Wang, S.; Zheng, Y.; Sen, S.; Chatterjee, A.; Thompson, P. R. Site-specific incorporation of citrulline into proteins in mammalian cells. *Nat. Commun.* **2021**, *12*, No. 45.
(37) Ite, K.; Yonezawa, K.; Kitanishi, K.; Shimizu, N.; Unno, M. Optimal mutant model of human S100A3 protein citrullinated at Arg51 by peptidylarginine deiminase type III and its solution structural properties. *ACS Omega* **2020**, *5*, 4032−4042.
(38) Takahara, H.; Oikawa, Y.; Sugawara, K. Purification and characterization of peptidylarginine deiminase from rabbit skeletal muscle. *J. Biochem.* **1983**, *94*, 1945−1953.
(39) Boyde, T. R. C.; Rahmatullah, M. Optimization of conditions for the colorimetric determination of citrulline, using diacetyl monoxime. *Anal. Biochem.* **1980**, *107*, 424−431.

NOTE ADDED AFTER ASAP PUBLICATION

This paper was published ASAP on August 8, 2022, with some of the data on incorrect lines in Table 1. The corrected version was reposted on August 16, 2022.

https://doi.org/10.1021/acsomega.2c02972
ACS Omega 2022, 7, 28378−28387